# Par3/Par6 polarity complex coordinates apical ectoplasmic specialization and blood–testis barrier restructuring during spermatogenesis

Elissa W. P. Wong*, Dolores D. Mruk*, Will M. Lee†, and C. Yan Cheng*‡

*Population Council, 1230 York Avenue, New York, NY 10065; and †School of Biological Sciences, University of Hong Kong, Pokfulam, Hong Kong

Edited by Ryuzo Yanagimachi, University of Hawaii, Honolulu, HI, and approved April 17, 2008 (received for review February 19, 2008)

**The Par3/Par6/aPKC and the CRB3/Pals1/PATJ polarity complexes are involved in regulating apical ectoplasmic specialization (ES) and blood–testis barrier (BTB) restructuring in the testis. Par6 was a component of the apical ES and the BTB. However, its level was considerably diminished at both sites at stage VIII of the cycle. Par6 also formed a stable complex with Pals1 and JAM-C (a component of the apical ES) in normal testes. When rats were treated with adjudin to induce apical ES restructuring without compromising the BTB, Par6 staining virtually disappeared at the apical ES in misaligned spermatids before their depletion. Additionally, the Par6/Pals1 complex became tightly associated with Src kinase, rendering a loss of association of the Par6/Pals1 complex with JAM-C, thereby destabilizing apical ES to facilitate spermatid loss. Primary Sertoli cell cultures with established functional BTB, but without apical ES, were next used to assess the Par6-based complex on BTB dynamics. When either Par6 or Par3 was knocked down by RNAi in Sertoli cell epithelium, a significant loss of the corresponding protein by ≈60% in cells vs. controls was detected, alongside with a decline in aPKC after Par6, but not Par3, knockdown. This Par3 or Par6 knockdown also led to a transient loss of selected BTB proteins at the cell–cell interface, thereby compromising the BTB integrity. These findings illustrate that the Par6/Par3-based polarity complex likely coordinates the events of apical ES and BTB restructuring that take place concurrently at the opposing ends of adjacent Sertoli cells in the seminiferous epithelium during spermatogenesis.**

The establishment and maintenance of polarity is essential for correct functioning of cells and tissues. Genetic analyses in *Caenorhabditis elegans* and *Drosophila melanogaster* have revealed a number of polarity complexes that control cell polarity in mammalian cells (1–3). Two of these complexes are the Crumb (CRB; CRB3/Pals1/PATJ) and the partitioning-defective (Par; Par3/Par6/aPKC) complexes. In recent years, the roles of the CRB and Par complexes in regulating cell polarity have been vigorously studied. Apart from regulating epithelial apical–basal polarity (1–3), these polarity complexes also play a role in other cellular events, such as directional cell migration (4). However, their involvement in regulating polarity and other cellular functions in mammalian tissues remains virtually unknown. In adult mammalian testes, spermatogenesis takes place in the seminiferous epithelium, which is composed of nondividing, differentiated, and polarized Sertoli cells that provide structural and nourishing supports to the dividing and differentiating germ cells (5, 6). Tight junctions (TJs), basal ectoplasmic specialization [ES; a testis-specific atypical adherens junction (AJ) type] and desmosome-like junctions are formed between adjacent Sertoli cells near the basement membrane that together constitute the blood–testis barrier (BTB) (7, 8). The BTB also segregates the seminiferous epithelium into the basal and apical compartments. During spermatogenesis, type B spermatogonia enter meiosis and differentiate into preleptotene/leptotene spermatocytes, which are the only germ cells that traverse the BTB at stage VIII of the epithelial cycle (9) and develop into elongating/elongated spermatids in the apical compartment. Interestingly, another ES called apical ES is present between elongating/elongated spermatids and Sertoli cells (7, 8). One of the major functions of the apical ES is to confer proper orientation of developing spermatids while maintaining their attachment on the Sertoli cells (5, 7, 8). Thus, in normal testes all of the elongating/elongated spermatids are arranged in a highly organized manner with their heads pointing toward the basement membrane. The apical ES, however, is disassembled at late-stage VIII to allow the release of fully developed elongated spermatids (i.e., spermatozoa) into the tubule lumen at spermiation (9). Interestingly, the disassembly of the apical ES during spermiation coincides with the transient "opening" or "restructuring" of the BTB to facilitate the transit of preleptotene/leptotene spermatocytes across the barrier. However, it remains a mystery how these two biological events are regulated and/or coordinated at the opposite ends of the same Sertoli cell. Using two established models in the field, we report findings that the CRB and Par complexes were involved in regulating these two concomitant events.

## Results

**Components of the CRB and Par Polarity Complexes in Rat Testes.** In mammalian cells, the CRB complex is composed of CRB3, Pals1, and PATJ, and the Par complex is constituted by Par3, Par6, and aPKC [supporting information (SI) Fig. S1]. Par6 is a key regulator of polarity because it binds directly to Pals1, providing cross-talk between the two polarity complexes (1–3). JAMs interact with Par3 (10, 11), and JAM-C is known to associate with the CRB and Par complexes in the testis (12) (Fig. S1). The component proteins of the CRB and Par complexes were found in testes, seminiferous tubules, and Sertoli and germ cells and their relative levels in Sertoli and germ cells are not identical (see Fig. S1).

**Par6 Is Localized at the Apical ES and BTB.** Par6 localization in the testis was examined by immunohistochemistry (IHC) by using frozen sections (Fig. 1*Aa*) with an anti-Par6 antibody (Table S1). Intense staining of Par6 was detected at the apical ES at the Sertoli-elongating spermatid interface (Fig. 1*A b* and *c*). Immunoreactive Par6 at the apical ES was observed in almost all stages of the epithelial cycle, except at late-stage VIII just before spermiation when its staining was greatly diminished (Fig. 1*A b* and *c* and *e* vs. *d*). Because Par6 is associated with TJ proteins in epithelial cells, we also investigated its localization at the BTB where TJs coexist with basal ES. As expected, strong Par6 staining was detected at the BTB in almost all stages of the epithelial cycle except that very weak signal was detected at stage VIII (Fig. 1*A f* vs. *g* and *h*). No specific

Author contributions: E.W.P.W., D.D.M., and C.-Y.C. designed research; E.W.P.W. and C.-Y.C. performed research; D.D.M., W.M.L., and C.-Y.C. contributed new reagents/analytic tools; E.W.P.W., and C.-Y.C. analyzed data; and E.W.P.W. and C.-Y.C. wrote the paper.

The authors declare no conflict of interest.

This article is a PNAS Direct Submission.

‡To whom correspondence should be addressed. E-mail: y-cheng@popcbr.rockefeller.edu.

This article contains supporting information online at www.pnas.org/cgi/content/full/0801527105/DCSupplemental.

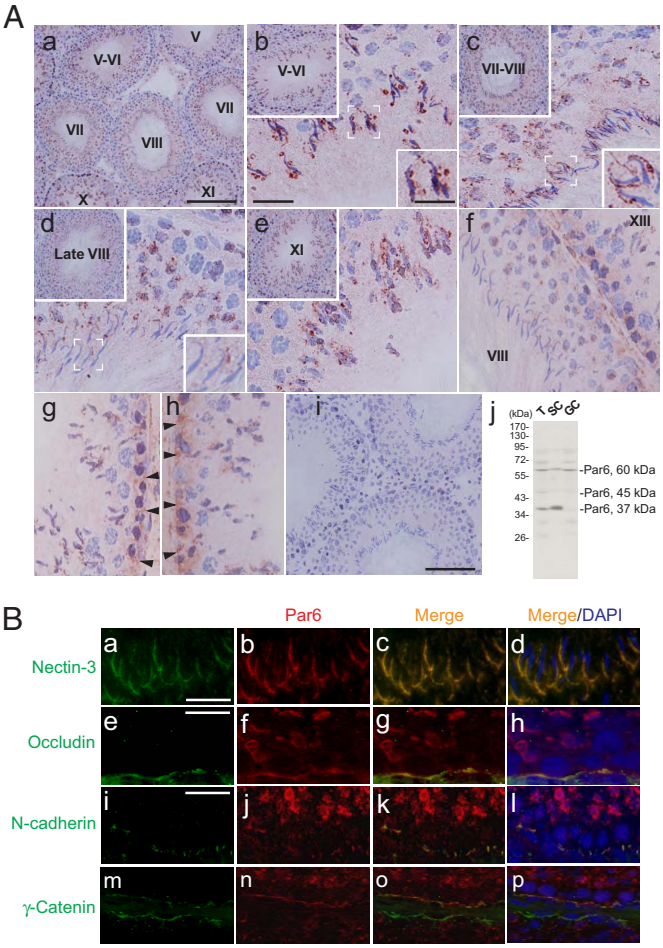


**Fig. 1.** Par6 is localized at the apical ES and BTB in adult rat testes. (*A*) (*a–h*) Frozen testis-sections were stained by using an anti-Par6 antibody (see Table S1) vs. control (*i*) stained with normal rabbit serum. (*a*) A low-magnification section of an adult rat testis is shown. (*b–e*) Magnified views of representative tubules at different stages of the epithelial cycle as shown in the *Upper Insets* at lower magnification. Par6 was localized at the apical ES (see *c* and the magnified area in *c Inset*) in almost all stages except that at late-stage VIII just before spermiation, it was greatly diminished (see *d* vs. *c*). *Lower Insets* in *b–d* are magnified views of the boxed regions. (*f–h*) Par6 was also localized prominently at the BTB sites (see black arrowheads in *g* and *h*) except that the Par6 staining at the BTB was also diminished at stage VIII (see *a* and *d* and *f* vs. *g* and *h*). (*j*) An immunoblot wherein 80 $\mu$g of protein from lysates of testis (T), Sertoli cell (SC), and germ cell (GC) was probed with an anti-Par6 antibody. [Scale bars: *a* (also applies to *Upper Insets* in *b–e*), 100 $\mu$m; *b* (also applies to *c–h*), 20 $\mu$m; *b Lower Inset* (also applies to *Lower Insets* in *c* and *d*), 10 $\mu$m; and *i*, 40 $\mu$m.] (*B*) Colocalization of Par6 (red) with apical ES protein nectin-3 (*a–d*, green) and BTB proteins [occludin (*e–h*), N-cadherin (*i–l*), and γ-catenin (*m–p*) (green)] was performed. Nuclei were stained with DAPI (blue). [Scale bars: *a* (also applies to *b–d*), 10 $\mu$m; *e* (also applies to *f–h*), 5 $\mu$m; and *i* (also applies to *j–p*), 10 $\mu$m.]

staining was observed when Par6 antibody was replaced with normal rabbit serum (Fig. 1*Ai*), illustrating the specificity of staining shown in Fig. 1*A*. Immunoblot analysis was performed by using lysates of testes, Sertoli, and germ cells detecting the three prominent bands of the Par6 isoforms at 37, 45, and 60 kDa, illustrating the specificity of the antibody (Fig. 1*Aj*). Double-labeled immunofluorescence analysis was subsequently used to examine colocalization of Par6 with different apical ES (nectin-3) and BTB (occludin, N-cadherin, γ-catenin) markers. At the apical ES, Par6 colocalized with nectin-3 (Fig. 1*B a–d*). Similarly, Par6 colocalized with TJ protein [occludin (Fig. 1*B e–h*)] and basal ES proteins [N-cadherin (Fig. 1*B i–l*) and γ-catenin (Fig. 1*B m–p*)] at the BTB.

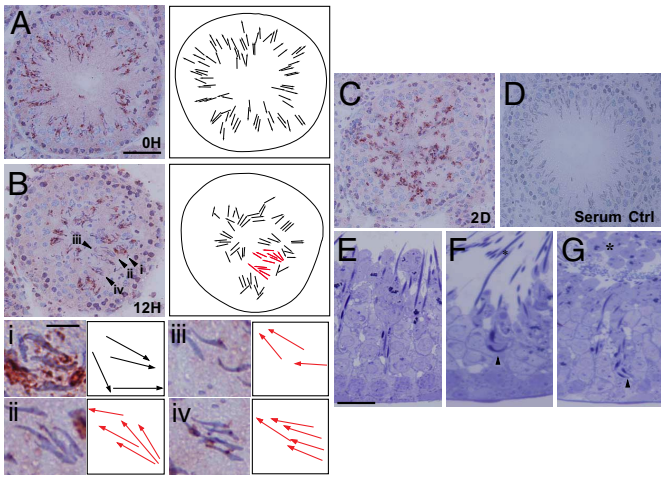


**Fig. 2.** Loss of Par6 at the apical ES in misoriented spermatids during adjudin-induced anchoring junction restructuring. (*A*) (*Left*) Normal testes were immunostained with an anti-Par6 antibody. Par6 was associated with elongating/elongated spermatids at the apical ES with spermatid heads pointing uniformly toward the basement membrane as illustrated schematically (*Right*). The black arrows depict the properly oriented spermatid heads maintained by the apical ES. (*B*) Twelve hours after adjudin treatment, groups of elongating/elongated spermatids were noted to become misoriented with their heads pointing toward the tubule lumen (red arrows in the schematic drawing, *Right*). Par6 staining associated with the misoriented spermatids was considerably diminished as seen in four randomly selected areas (denoted by black arrowheads) which were enlarged and shown in *i–iv* for comparison between correctly (*i*) or incorrectly (*ii–iv*) oriented spermatids. (*C*) Nearly all elongating/elongated spermatids were depleted from the epithelium by 2 days after adjudin treatment and found in the lumen with Par6 still associated with spermatids. (*D*) Control section using normal rabbit serum instead of anti-Par6 antibody. (*E–G*) Semithin testis sections illustrating a representative stage VI tubule from normal testes (*E*) and 12 h after adjudin treatment (*F* and *G*). Spermatids were found in the tubule lumen (see asterisk in *F* and *G*) but absent in normal testes (*E* vs. *F* and *G*), and misaligned spermatids were found in the epithelium (see black arrowheads in *F* and *G*). [Scale bars: *A* (also applies to *B–D*), 80 $\mu$m; *i* (also applies to *ii–iv*), 10 $\mu$m; and *E* (also applies to *F–G*), 8 $\mu$m.]

**Changes in Steady-State Levels of Polarity Complexes During Adjudin-Induced Germ Cell Loss.** We speculated that the reduced level of Par6 at both the apical ES and BTB at late-stage VIII of the epithelial cycle detected by IHC might regulate the events of apical ES disassembly at spermiation and the BTB restructuring to facilitate spermatocytes in transit at the BTB. To address whether Par6 is a regulator of apical ES dynamics, an *in vivo* animal model was used. Adult rats treated with adjudin were shown to deplete germ cells from the seminiferous epithelium as a result of extensive AJ restructuring without compromising the BTB integrity (5). This *in vivo* model thus serves to study AJ dynamics, in particular the apical ES (5, 13, 14). Testis lysates were obtained from rats treated with adjudin for immunoblot analysis. Results shown in Fig. S2 suggest that the loss of Par6 at the apical ES in adjudin-induced misaligned spermatids detected by IHC (Fig. 2) is not likely caused by a reduced steady-state level of Par6 in the testis. Instead, this loss appears to be the result of an alteration in protein distribution and/or protein–protein association that impedes germ cell adhesion.

**Loss of Par6 Staining in Misoriented Spermatids.** Because the significant decline in the steady-state Par6 protein level at 4 days after adjudin treatment (see Fig. S2) might be caused by a reduced contribution by germ cells, we thus selected two earlier time points (12 h and 2 days) after adjudin treatment to investigate the *in situ* localization of Par6 before massive germ cell loss occurred (Fig. 2 *A–D*). Par6 in normal testis section was mostly associated with

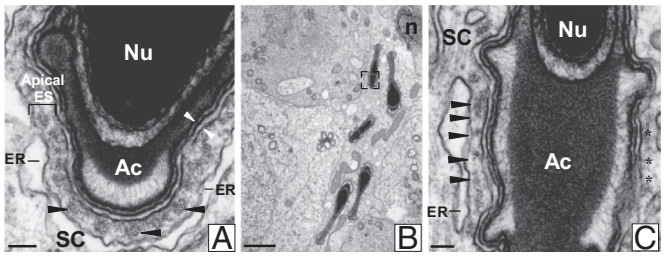


**Fig. 3.** Adjudin-induced misorientation of elongating spermatids and ultrastructural changes at the apical ES. (*A*) An electron micrograph from a normal rat testis showing an elongating spermatid (Nu, nucleus; Ac, acrosome) anchored onto a Sertoli cell (SC) in which the actin filament bundles (black arrowheads) were sandwiched between cisternae of endoplasmic reticulum (ER) and two apposing plasma membranes of Sertoli and germ cells (see apposing white arrowheads). (*B*) The Sertoli cell nucleus (n) located near the basement membrane is clearly visible in this testis 12 h after adjudin treatment, with the heads of two misoriented elongating spermatids pointing toward the tubule lumen, one of these is boxed and magnified in *C*. (*C*) The actin filament bundles at the apical ES were either defragmenting (see black arrowheads) or already disintegrated (see asterisks). (Scale bars: *A*, 0.1 $\mu$m; *B*, 2 $\mu$m; and *C*, 0.1 $\mu$m.)

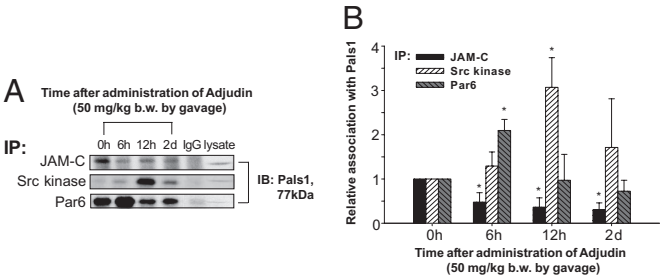


**Fig. 4.** Changes in the association of Pals1 with polarity proteins during adjudin-induced spermatid misorientation. (*A*) Testes lysates (700 $\mu$g) from rats treated with adjudin at specified time points were used for Co-IP with an anti-JAM-C, anti-Src kinase or anti-Par6 antibody and immunoblotted with an anti-Pals1 antibody. A decrease in protein–protein association between JAM-C and Pals1 was observed by 6 h after adjudin treatment when elongating/elongated spermatids began to undergo misorientation. An increase in protein–protein association for Par6–Pals1 and Src kinase–Pals1 was detected at 6 and 12 h, respectively. (*B*) This histogram illustrates the composite results of three independent sets of experiments. Protein–protein association at 0 h was arbitrarily set at 1. Each bar is mean ± SD. *, $P < 0.05$ by one-way ANOVA.

elongating/elongated spermatids at the apical ES (Fig. 2*A*) in all stages except late-stage VIII of the epithelial cycle. In addition, all elongating spermatids were properly oriented in the epithelium with their heads pointing toward the basement membrane (Fig. 2*A Right*, arrows pointing toward the basement membrane in each tubule). This proper spermatid orientation is known to be maintained by the apical ES (5). Interestingly, at 12 h after adjudin treatment, groups of elongating/elongated spermatids were misoriented with their heads pointing toward the tubule lumen (Fig. 2*B Right*, red arrows, misoriented elongating spermatids vs. black arrows, properly oriented elongated spermatids). This observation was validated by comparing the epithelium of adjudin-treated rats at 12 h by using semithin sections (see stage VI tubules in Fig. 2 *E–G*), where elongating spermatids were depleting from the epithelium vs. controls (Fig. 2 *F* and *G* vs. *E*). Misaligned spermatids were visible in the epithelium (see arrowheads in Fig. 2 *F* and *G* vs. *E*), and these misoriented spermatids were associated with a significant decrease in Par6 staining (Fig. 2*B ii–iv* vs. *i*). After the more advanced elongating/elongated spermatids were depleted from the epithelium by 2 days, Par6 was still associated with the remaining spermatids at the apical ES (Fig. 2*C*). By using electron microscopy (Fig. 3), misoriented spermatids were clearly visible (Fig. 3*B*), and the apical ES of a typical misaligned spermatid was magnified (see the boxed spermatid in Fig. 3*B*, with the head pointing away from the basement membrane, where the Sertoli cell nucleus, n, is located) and shown in Fig. 3*C*. In normal testes (Fig. 3*A*), apical ES is typified by the presence of actin filament bundles (black arrowheads) sandwiched between endoplasmic reticulum (ER) and the two apposing plasma membranes of Sertoli and elongating spermatid (apposing white arrowheads). In the misoriented elongating spermatid (Fig. 3*C*), actin bundles were either defragmenting (black arrowheads) or absent (asterisks) at the apical ES.

**Pals1–Par6 Complex Is Sequestered from JAM-C to Associate with Src Kinase: A Prerequisite of Germ Cell Depletion from the Epithelium?** Because the overall protein level of Par6 in the testes did not change significantly between 0 h and 2 days postadjudin treatment (see Fig. S2 *A–F*), we sought to examine whether there were any changes in protein–protein interactions by coimmunoprecipitation (Co-IP) among the polarity proteins that might have led to the loss of Par6 at the apical ES, such as via protein redistribution in misoriented spermatids as shown in Fig. 2*B*. Using an anti-JAM-C antibody for Co-IP, immunoblotting was performed with anti-Pals1 antibody (Fig. 4*A*). The results of three independent experiments were shown in Fig. 4*B*. A significant loss of protein–protein association between JAM-C and Pals1 was detected starting from 6 h, and this decrease in association persisted up to 2 days (Fig. 4) when the steady-state level of JAM-C in these testes lysates remained constant (Fig. S2 *A–F*). On the other hand, when anti-Src kinase or anti-Par6 antibody was used for IP and the resultant immunocomplexes were used for immunoblotting with anti-Pals1, a significant increase in protein–protein association between Src kinase and Pals1 or between Par6 and Pals1 was detected at 12 and 6 h, respectively. This time corresponded to when germ cells began to misalign before their depletion from the epithelium (Fig. 4). These results suggest that the tighter association among Par6, Pals1, and Src kinase may actually sequester Pals1 and probably Par6 from JAM-C at the apical ES site, leading to a loss of Pals1/Par6 at the apical ES. This, in turn, may destabilize the JAM-C-based adhesion, leading to elongating/elongated spermatid loss from the epithelium.

**Loss of Par6 Causes a Decrease in the Steady-State Levels of aPKC and BTB-Associated Proteins.** Primary Sertoli cell cultures have been used as an *in vitro* model to study BTB dynamics because Sertoli cells assemble functional TJ and basal ES *in vitro*, which mimic the BTB *in vivo*, including the ultrastructural features (14–16). As shown in Fig. 5*A*, Sertoli cells formed visible BTB structures with a functional TJ-permeability barrier, which was confirmed by quantifying the transepithelial electrical resistance (TER) across the cell epithelium (Fig. 5*B*). These cultures were then used for subsequent RNAi experiments. To determine the function of Par6 on BTB dynamics, Par6 was knocked down by transfecting Sertoli cells with a siRNA duplex specific for Par6$\alpha$. The only Par6$\alpha$ detected in Sertoli cells was at 37 kDa (Fig. S1*C*). Cells transfected with nontargeting siRNA served as control. Immunoblot analysis showed that only the 37-kDa Par6 in Sertoli cells, but not the 60-kDa Par6, was reduced by ≈60% when compared with nontargeting siRNA controls illustrating the specificity and the effectiveness of the silencing (Fig. 5 *C* and *D*). The steady-state protein levels of aPKC and selected BTB-associated proteins such as those found at the TJ (e.g., occludin, JAM-A and ZO-1) and basal ES (e.g., N-cadherin, $\alpha$-catenin, $\beta$-catenin, and $\gamma$-catenin) were examined by immunoblotting using lysates from Par6 knockdown cells. In Par6-depleted cells, the protein levels of aPKC, N-cadherin, and $\gamma$-catenin were significantly reduced, with a mild but statistically insignificant reduction in JAM-A, but no change in other BTB proteins examined in our study (Fig. *C–E*). When cells were transfected with specific Par3 siRNA duplex to knock down all three Par3 isoforms (100, 150, and 180 kDa), no significant change in the protein levels

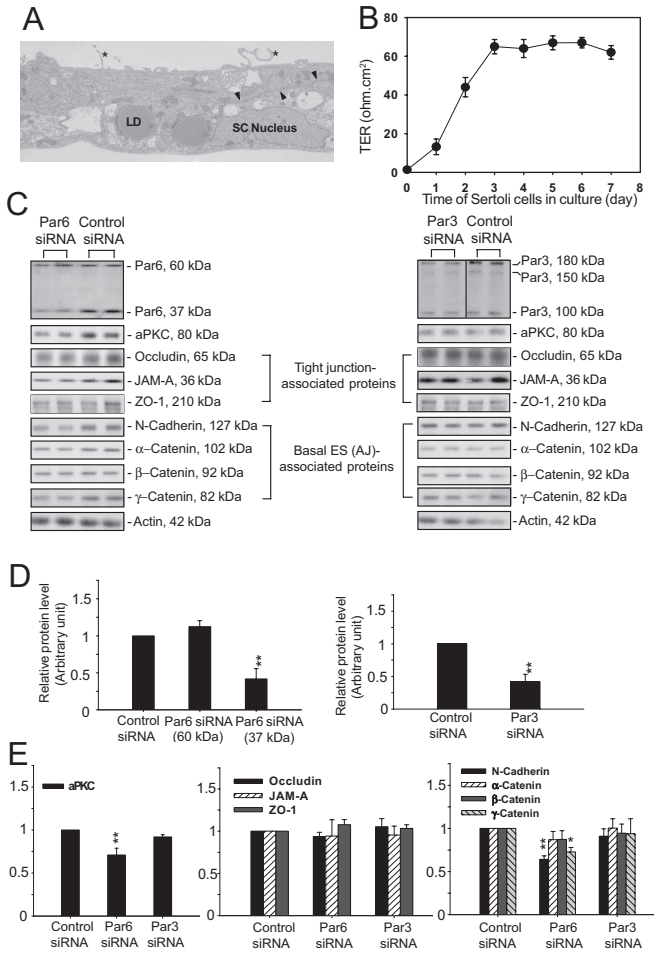


**Fig. 5.** Knockdown of Par6 in Sertoli cells results in changes in the steady-state proteins levels of aPKC and BTB-associated proteins. (*A* and *B*) Sertoli cells, such as those used for RNAi experiments (see below), were cultured for 3 days with functional BTB [arrowheads; and the finger-like cytoplasmic processes (asterisks), which are typical features of Sertoli cells cultured *in vitro* (*A*)], which was confirmed by quantifying TER across the cell epithelium on Matrigel-coated bicameral units (*B*). Data are mean ± SD of $n = 3$. SC, Sertoli cell; LD, lipid droplet. (*C*) Par6 or Par3 was knocked down by transfecting cells with specific siRNA duplex against Par6 or Par3 vs. control siRNA duplex and analyzed by immunoblotting 4 days thereafter, illustrating Par6 or Par3 was knocked down by ≈60% vs. control. Note that the Par6 siRNA duplex was directed against the 37-kDa isoform only, whereas the Par3 siRNA duplex was against all three Par3 isoforms (100, 150, and 180 kDa). (*D* and *E*) These histograms are composite results of data such as those shown in *C* normalized against actin. Relative protein levels of control siRNA were arbitrarily set at 1 against which statistical analysis was performed. Each bar is mean ± SD of $n = 3$. *, $P < 0.05$; **, $P < 0.01$.

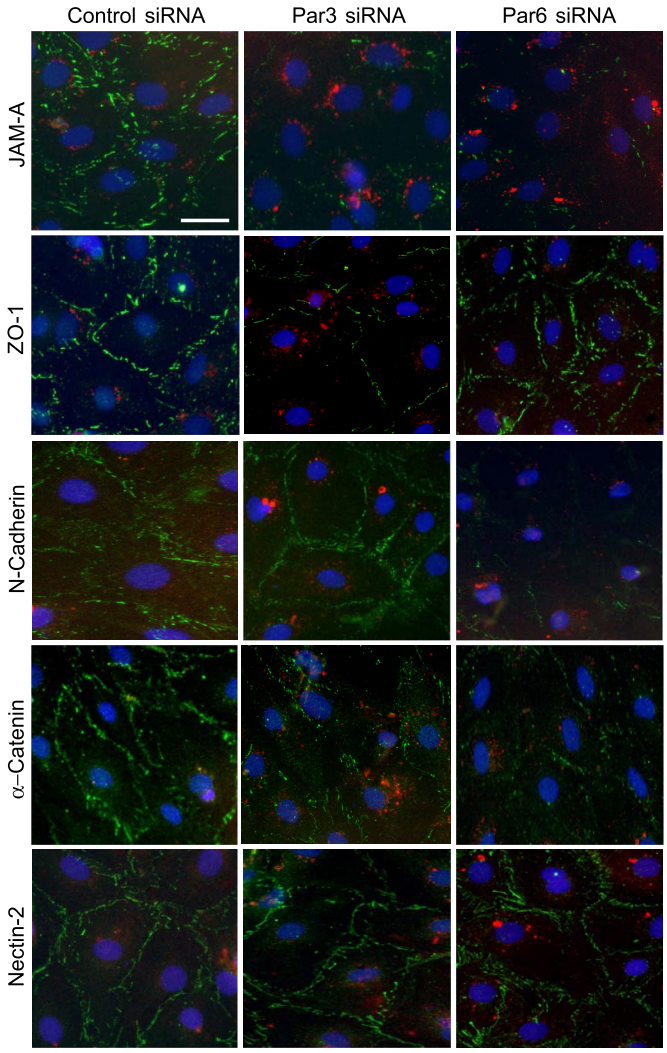


**Fig. 6.** Normal protein distribution at the Sertoli–Sertoli cell interface is disrupted after knockdown of Par3 or Par6. Primary Sertoli cells were transfected with Cy3-labeled (red) nontargeting control (*Left*), Par3 siRNA duplex (*Center*), or Par6 siRNA duplex (*Right*). Two days after transfection, cells were subjected to calcium switch by first starving cells in DMEM without growth factors for 1 h followed by incubation in medium with 4 mM EGTA for 3 h and returned to normal DMEM with growth factors for 7 h. Cells were stained with the indicated TJ and basal ES markers (green) at the BTB. Loss of Par3 and Par6 resulted in a disruption of JAM-A and α-catenin at the cell–cell contact sites. Silencing of Par6 and Par3 also caused a loss of N-cadherin and ZO-1 at the cell–cell contact sites, respectively. (Scale bar: 5 μm.)

for aPKC or other BTB-associated proteins was observed even though the endogenous Par3 protein level in the transfected cells was reduced by ≈60% (Fig. 5 *C–E*).

**Junction Disruption at the Sertoli–Sertoli Cell Interface After Par6 and Par3 Knockdown.** We next investigated whether the knockdown of Par6 or Par3 in Sertoli cells affected the proper localization of BTB-associated proteins at the cell–cell interface. Nontargeting siRNA and siRNA directed specifically against Par6 or Par3 were labeled with Cy3 and appeared as red fluorescence in transfected cells. Two days after transfection, Sertoli cells were subjected to calcium switch and stained for JAM-A, ZO-1, N-cadherin, α-catenin, and nectin-2 (Fig. 6). Cells transfected with nontargeting siRNA displayed normal localization of all of the junction proteins examined at the cell–cell interface (Fig. 6). These results in control cultures also verified the establishment of TJ and basal ES in Sertoli cell culture. In Par6 or Par3 knockdown cells, staining results showed that JAM-A failed to localize at the cell junction site (Fig. 6). Similar changes were observed for α-catenin when Par6 or Par3 was depleted (Fig. 6). Knockdown of Par6, but not Par3, also resulted in reduced immunofluorescence signal of N-cadherin, which was consistent with the reduction of the N-cadherin protein level after depletion of Par6 (Fig. 5 *C* and *E*). On the other hand, ZO-1 was mislocalized when Par3, but not Par6, was knocked down (Fig. 6). The localization of nectin-2 at the cell–cell adhesion site, however, was not affected by either Par3 or Par6 knockdown (Fig. 6).

## Discussion

The involvement of CRB and Par proteins in regulating TJ and epithelial polarity in cell lines and *Drosophila* is well established

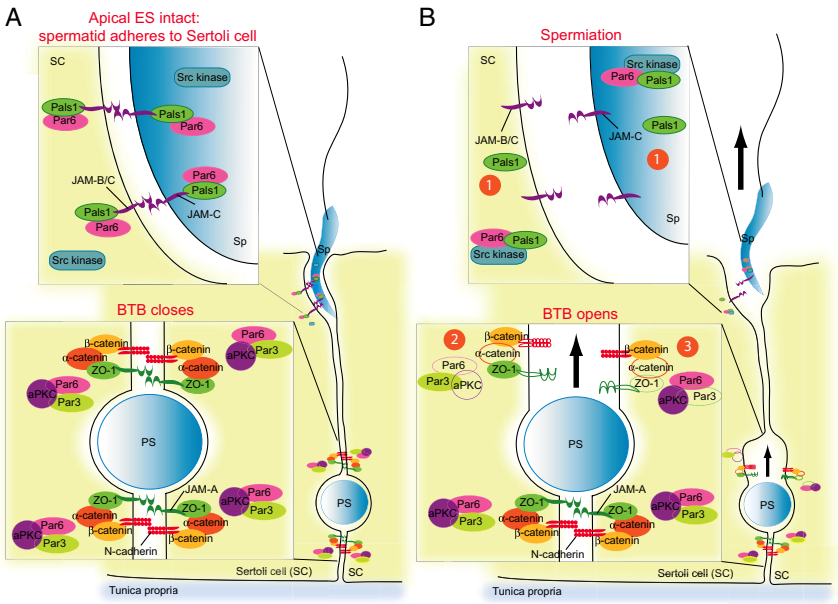


**Fig. 7.** A hypothesis depicting the regulation of apical ES and BTB restructuring by Par3/Par6 at stage VIII of the epithelial cycle. (*A*) At the apical ES before spermiation, Par6/Pals1 forms an adhesion complex with JAM-C to facilitate spermatid attachment to Sertoli cells. The presence of the Par3/Par6/aPKC complex also facilitates BTB closure by stabilizing the N-cadherin- and JAM-C-based adhesion complexes. (*B*) Par3 and Par6 possibly regulate the disassembly of apical ES and BTB at stage VIII of the epithelial cycle as follows: (1) At the apical ES, the tighter association among Pals1, Src kinase, and Par6 (may also be coupled with a transient loss and/or redistribution of Par6) plausibly sequesters the polarity protein complexes from JAM-C, destabilizing the JAM-C adhesion complex, leading to spermiation. (2) When the level of Par6 at the BTB is down-regulated, such as by cytokines, this leads to a decrease in aPKC level. Subsequently, N-cadherin, α-catenin, and JAM-A are degraded or endocytosed, leading to a transient BTB opening to facilitate the transit of preleptotene spermatocytes (PS) across the BTB. (3) Similarly, down-regulation of Par3 results in redistribution of junction proteins (α-catenin, ZO-1, and JAM-A) via endocytosis or degradation, destabilizing the BTB, contributing to its opening. Unshaded target proteins represent molecules that are either degraded or endocytosed. Sp, elongated spermatid.

(1–3). However, little is known regarding their roles in regulating AJ. Nonetheless, a recent report (17) has shown that Par3 is likely to be involved in forming cadherin-based, but not nectin-based, AJs in epithelial cells. Our results reported herein using the testis as a model further strengthens the notion regarding the involvement of Par proteins in AJ function. Studies by IHC have illustrated that Par6 is found at the apical ES and colocalized with a putative apical ES marker, nectin-3. Interestingly, Par6 staining is not visible at the apical ES just before the mature elongated spermatids detach from the seminiferous epithelium at spermiation. This finding seemingly suggests that a loss of Par6 at the apical ES is necessary for its disassembly at spermiation. This notion is supported by the *in vivo* observation that Par6 staining is also greatly diminished at the apical ES in elongating spermatids before their depletion from the epithelium when induced by adjudin. Unexpectedly, this adjudin-induced anchoring junction restructuring is associated with a misorientation of elongating spermatids and a loss of Par6 staining at the apical ES. One of the major functions that was ascribed to apical ES based on morphological study is to orientate developing spermatids properly in the epithelium during their development (5, 8), with their heads pointing toward the basement membrane, until they are released into the tubular lumen at spermiation. These findings thus provide evidence that the Par6-based protein complex at the apical ES is crucial to maintain proper orientation of developing spermatids.

In addition, when developing spermatids were found to misorientate in the epithelium at ≈6–12 hr after adjudin treatment, this event was associated with a change in interactions among the polarity proteins and JAM-C. For instance, starting from 6 h after adjudin administration, spermatids were shown to misorientate in the epithelium when the association between JAM-C and Pals1 was significantly reduced. JAM-C is an integral membrane protein at the apical ES in rodents and humans that confers cell adhesion. It has been suggested that JAM-B in Sertoli cells and JAM-C in germ cells form heterophilic interaction to confer adhesion function at the apical ES (12). However, our results have demonstrated that there is a relatively little, yet detectable, amount of JAM-C in primary Sertoli cell cultures with negligible germ cell contamination. Thus it is possible that JAM-C in Sertoli cells also forms a homophilic interaction with JAM-C in germ cells to confer cell adhesion at the apical ES. On the other hand, a significant increase in association between Par6 and Pals1 as well as Src kinase and Pals1 was detected at 6 and 12 h postadjudin treatment, respectively, with a concomitant loss in association with JAM-C. On the basis of these findings, we propose in Fig. 7 that the JAM-C-based adhesion complex at the apical ES that confers cell adhesion forms a stable complex with the Pals1/Par6 polarity proteins. When the apical ES undergoes restructuring, such as during spermiation or adjudin-induced spermatid loss, an increase in association among Src kinase, Pals1, and Par6 pulls the polarity proteins away from the JAM-C adhesion complex. This in turn destabilizes the JAM-C-mediated adhesion that leads to spermatid depletion from the epithelium. This hypothesis explains the loss of Par6 staining in misoriented spermatids at the apical ES becausePar6 is possibly pulling away from the apical ES site by Pals1 and Src kinase. This model is also supported by the observations that overexpression of Lethal giant larvae (Lgl) (18) or VE-cadherin (19), two proteins known to interact with Par6, resulted in a disruption of TJs in epithelial cells, possibly because of the sequestration of Par6 protein from the TJ.

In this report, we also provide evidence that Par6 and Par3 regulate the transient opening of the BTB. It is known that Par proteins are involved in TJ assembly. For instance, silencing of Par3 in mammalian epithelial cells results in defects in TJ assembly, including mislocalization of TJ markers, such as occludin and ZO-1, and delay in TJ barrier formation (20). Consistent with these earlier findings, a loss of Par3 or Par6 in Sertoli cell cultures with established TJ barrier and the ultrastructural features of the BTB *in vivo* was shown to induce disrupted localization of TJ proteins such as JAM-A at the cell–cell interface. This observation is also likely to be attributed to the fact that Par3 is structurally associated with JAMs (10, 21). The differential disruption of junction proteins at the cell–cell interface after loss of Par6 and Par3 thus prompts us to speculate that they may work in concert to regulate the restructuring of the BTB to facilitate germ cell movement while maintaining its integrity (Fig. 7). We note that the distribution of nectin-2 at the cell–cell junction in these knockdown experiments was not affected, which is not surprising as Par proteins are likely to be involved in regulating cadherin-based, but not nectin-based, AJs (17). Earlier studies have shown that a blockade of the α6β1-integrin–laminin-333 function at the apical ES by the use of anti-laminin β3 or γ3 IgG could impede both spermatid adhesion at the apical ES *and* BTB function (22), and specific fragments of laminin γ3 could perturb the Sertoli cell TJ barrier *in vitro* either

directly at the BTB or via hemidesmosome (23). However, it was not known at the time how the signal could be transduced between apical ES and BTB because these ultrastructures are present at the opposite end of the Sertoli cell epithelium. The fact that the $\alpha 6\beta 1$-integrin–laminin-333 protein complex was shown to interact with Src kinase (22), which also has been shown to associate with the Par3/Par6 polarity complex as reported here, seemingly suggests that this polarity complex can serve as a "molecular switch" that mediates signals between the apical ES and the BTB. In short, Par proteins are regulators and/or coordinators of (*i*) spermiation that occurs at late-stage VIII, and (*ii*) BTB restructuring to facilitate spermatocyte transit that occurs at stages VIII-IX of the epithelial cycle.

## Materials and Methods

**Animals and Antibodies.** The use of Sprague–Dawley rats was approved by the Rockefeller University Animal Care and Use Committee (protocol no. 06018). Antibodies were obtained commercially (see Table S1).

**Induction of Germ Cell Loss from the Seminiferous Epithelium *in Vivo* by Adjudin [1-(2,4-dichlorobenzyl)-*1H*-indazole-3-carbohydrazide].** Adult rats [≈ 300 g body weight (b.w.)] were treated with a single dose of adjudin (50 mg/kg b.w. by gavage), which is known to induce anchoring junction restructuring in the seminiferous epithelium, leading to premature germ cell loss, most notably elongating/elongated spermatids (5). Rats were euthanized by $CO_2$ asphyxiation at specified time points ($n = 3$ for each time points). In selected experiments, testes were perfused with 0.05 M sodium cacodylate buffer (pH 7.4 at 22°C) containing 4% paraformaldehyde (vol/vol), 2.5% glutaraldehyde (vol/vol), and 0.05% picric acid (vol/vol) and embedded in epon for semithin sections. Electron microscopy was performed at the Rockefeller University BioImaging Resource Center as described (22).

**IHC and Immunofluorescent Microscopy.** IHC and immunofluorescent microscopy were performed as described (13, 14). Controls include testis sections incubated with either normal rabbit IgG or normal rabbit serum. To minimize inter-experimental variations, all sections within an experimental set were processed simultaneously. All images were acquired by using QCapture software (Quantitative Imaging) with an Olympus BX40 fluorescent microscope and an Olympus DP70 12.5MPa digital camera.

**Primary Cell Cultures and Transfection of Sertoli Cells with siRNA.** Primary Sertoli cells were isolated from 20-day-old rat testes as described (14). Cells were plated at a density of $0.5 \times 10^6$ cells/cm$^2$ on 12-well dishes coated with Matrigel [Matrigel/F12/DMEM at 1:7 (vol/vol); BD Biosciences]. Hypotonic treatment was performed 2 days after isolation (24) to lyse residual germ cells. Thus, these Sertoli cell cultures had a purity of >98% and were contaminated with negligible germ, Leydig, and peritubular myoid cells by using corresponding specific cell markers (26). Two days thereafter, cells were transfected with 100 nM siRNA by using 4 $\mu$l of TransIT-TKO transfection reagent (Mirus Bio) in a final sample volume of 1 ml. Cells were cultured in F12/DMEM supplemented with different growth factors for 3 days and transfected again 24 h before their harvest for cell lysate preparation by using the IP lysis buffer [50 mM Tris, 150 mM NaCl, 1% Nonidet P-40 (vol/vol), 2 mM EGTA, 2 mM ethylmaleimide, 10% glycerol (vol/vol), pH 7.4 at 22°C, freshly supplemented with 1 $\mu$g/ml aprotinin, 1 $\mu$g/ml leupeptin, 2 mM PMSF, and 1 mM sodium orthovanadate]. To silence Par3, rat Pard3 (NM_031235) duplex 2 of 5′-AGGUAUAGCUGACGAGACUUU (J-097288-10) was used (siGENOME ON-TARGET plus; Dharmacon). A mixture of two duplexes, rat Pard6a (NM_001003653) duplex 1 of 5′-GGGAAUGGCAUGCGAGGUGUU (J-102296-05) and duplex 4 of 5′-GCAGAGAGCAAGCCAAUUCUU (J-102296-08) (siGENOME ON-TARGET plus; Dharmacon) were used to silence Par6. ON-TARGET plus siCONTROL nontargeting pool siRNA was used as control (D-001810–10; Dharmacon). For cell staining after RNAi, Sertoli cells were plated on 100-mm culture dishes at a density of $0.05 \times 10^6$ cells/cm$^2$. Two days after isolation, transfection was performed essentially the same as described above except that 80 nM siRNA was used. siRNA was fluorescently labeled by using a LabelIT siRNA Tracker Cy3 kit (Mirus Bio) to track transfected cells with red fluorescence. Two days after transfection, cells were subjected to calcium switch before staining. Calcium switch was performed as described (17) with minor modifications. In short, cells were washed with F12/DMEM twice and starved in F12/DMEM without growth factors for 1 h. Cells were then cultured in F12/DMEM with growth factors and 4 mM EGTA for 3 h to chelate $Ca^{2+}$. To allow the re-establishment of the TJ barrier, cells were washed twice with F12/DMEM without EGTA before returning to F12/DMEM with growth factors for an additional 7 h. Cells were washed twice with PBS, fixed with ice-cold methanol at −20°C for 10 min, and examined by fluorescence microscopy.

**TER Measurement.** Sertoli cells cultured *in vitro* formed functional BTB with the ultrastructural features of TJ and basal ES when examined by electron microscopy (14) and TER across the cell epithelium (23). The presence of functional BTB in cultures used for silencing experiments was assessed in selected experiments as described (14, 23).

**General Methods.** Immunoblotting, Co-IP, and statistical analysis were performed as described in SI *Materials and Methods*.

**ACKNOWLEDGMENTS.** We thank Ms. Eleana Sphicas at the Rockefellar University BioImaging Resource Center for her excellent technical assistance in electron microscopy. This work was supported in part by National Institutes of Health Grants NICHD U01 HD045908 and R03 HD051512; Hong Kong Research Grants Council (HKU 7693/07M), and the University of Hong Kong CRCG Seed Funding.

1. Macara IG (2004) Parsing the polarity code. *Nat Rev Mol Cell Biol* 5:220–231.
2. Shin K, Fogg VC, Margolis B (2006) Tight junctions and cell polarity. *Annu Rev Cell Dev Biol* 22:207–235.
3. Suzuki A, Ohno S (2006) The Par-aPKC system: Lessons in polarity. *J Cell Sci* 119:979–987.
4. Shin K, Wang Q, Margolis B (2007) PATJ regulates directional migration of mammalian epithelial cells. *EMBO J* 8:158–164.
5. Mruk DD, Cheng CY (2004) Sertoli–Sertoli and Sertoli–germ cell interactions and their significance in germ cell movement in the seminiferous epithelium during spermatogenesis. *Endocr Rev* 25:747–806.
6. de Krester DM, Kerr JB (1988) The cytology of the testis. *The Physiology of Reproduction*, eds Kobil E, *et al.* (Raven, New York), pp 837–932.
7. Wong EWP, Mruk DD, Cheng CY (2008) Biology and regulation of ectoplasmic specialization, an atypical adherens junction type, in the testis. *Biochim Biophys Acta* 1778:692–708.
8. Vogl AW, Pfeiffer DC, Mulholland D, Kimel G, Guttman J (2000) Unique and multifunctional adhesion junctions in the testis: Ectoplasmic specializations. *Arch Histol Cytol* 63:1–15.
9. Russell LD (1977) Movement of spermatocytes from the basal to the adluminal compartment of the rat testis. *Am J Anat* 148:301–312.
10. Itoh M, *et al.* (2001) Junctional adhesion molecule (JAM) binds to Par-3: A possible mechanism for the recruitment of Par-3 to tight junctions. *J Cell Biol* 154:491–497.
11. Ebnet K, *et al.* (2003) The junctional adhesion molecule (JAM) family members JAM-2 and JAM-3 associate with the cell polarity protein Par-3: A possible role for JAMs in endothelial cell polarity. *J Cell Sci* 116:3879–3891.
12. Gliki G, Ebnet K, Aurrand-Lions M, Imhof BA, Adams RH (2004) Spermatid differentiation requires the assembly of a cell polarity complex downstream of junctional adhesion molecule C. *Nature* 431:320–324.
13. Yan HHN, Cheng CY (2005) Blood–testis barrier dynamics are regulated by an engagement/disengagement mechanism between tight and adherens junctions via peripheral adaptors. *Proc Natl Acad Sci USA* 102:11722–11727.
14. Siu MK, Wong CH, Lee WM, Cheng CY (2005) Sertoli-germ cell anchoring junction dynamics in the testis are regulated by an interplay of lipid and protein kinases. *J Biol Chem* 280:25029–25047.
15. Byers S, Hadley MA, Djakiew D, Dym M (1986) Growth and characterization of epididymal epithelial cells and Sertoli cells in dual environment culture chambers. *J Androl* 7:59–68.
16. Janecki A, Steinberger A (1986) Polarized Sertoli cell functions in a new two-compartment culture system. *J Androl* 7:69–71.
17. Ooshio T, *et al.* (2007) Cooperative roles of Par-3 and afadin in the formation of adherens and tight junctions. *J Cell Sci* 120:2352–2365.
18. Yamanaka T, *et al.* (2003) Mammalian Lgl forms a protein complex with Par-6 and aPKC independently of Par-3 to regulate epithelial cell polarity. *Curr Biol* 13:734–743.
19. Iden S, *et al.* (2006) A distinct Par complex associates physically with VE-cadherin in vertebrate endothelial cells. *EMBO Rep* 7:1239–1246.
20. Chen X, Macara IG (2005) Par-3 controls tight junction assembly through the Rac exchange factor Tiam1. *Nat Cell Biol* 7:262–269.
21. Ebnet K, *et al.* (2001) The cell polarity protein ASIP/Par-3 directly associates with junctional adhesion molecule (JAM). *EMBO J* 20:3738–3748.
22. Yan HHN, Cheng CY (2006) Laminin $\alpha 3$ forms a complex with $\beta 3$ and $\gamma 3$ chains that serves as the ligand for $\alpha 6\beta 1$-integrin at the apical ectoplasmic specialization in adult rat testes. *J Biol Chem* 281:17286–17303.
23. Yan HHN, Mruk DD, Wong EWP, Lee WM, Cheng CY (2008) An autocrine axis in the testis that coordinates spermiation and blood–testis barrier restructuring during spermatogenesis. *Proc Natl Acad Sci USA* 105:8950–8955.
24. Galdieri M, Ziparo E, Palombi F, Russo MA, Stefanini M (1981) Pure Sertoli cell cultures: A new model for the study of somatic-germ cell interactions. *J Androl* 5:249–259.